COMPARATIVE ASSESSMENT OF PREDICTIVE CONTROLLERS FOR AN INVERTED PENDULUM WITH THREE CONFLICTING CONTROL OBJECTIVES

Adilson de Souza Cândido
Roberto Kawakami Harrop Galvão
Takashi Yoneyama
Instituto Tecnológico de Aeronáutica, São José dos Campos, Brasil

Abstract. *Model predictive control (MPC) designates a class of moving-horizon optimal control techniques based on the use of a process model to make predictions of the plant output. Over the past 30 years, several MPC formulations have been reported in the literature. These formulations differ from each other mainly in the type of process and disturbance models adopted, as well as in the cost function to be minimized. Given a specific problem, the selection of the most appropriate MPC approach may not be straightforward. In fact, control tasks usually involve multiple conflicting objectives, which cannot be easily combined in a single performance index for comparative assessment of different control laws. Moreover, the proper use of MPC requires the tuning of several design parameters such as horizon lengths and cost function weights. Therefore, a fair comparison between predictive controllers can only be carried out if they have been suitably tuned with respect to the control objectives under consideration. This paper presents a multi-objective approach for comparison of control strategies employing the concepts of dominance and Pareto optimality. This approach is illustrated in a simulated case study involving the control of an inverted pendulum coupled to a cart. Three conflicting objectives are considered, namely (1) fast response to setpoint changes in the cart position, (2) robustness with respect to model uncertainties and (3) low sensitivity to sensor noise. Two different MPC formulations are compared in terms of their Pareto boundaries for these three objectives. The results show that the proposed approach may be a useful aid in the selection and tuning of appropriate controllers for a given task.*

Keywords: *Inverted pendulum, model predictive control, multi-objective optimization, Pareto boundary*

1. INTRODUCTION

The control and regulation of an inverted pendulum on a cart is a benchmark problem in control systems theory. This plant is naturally unstable with fast, nonlinear and strongly coupled multivariable dynamics. Because of those characteristics, the inverted pendulum system is often used to verify the effectiveness of control techniques (Wu and Liu, 2007). Along the years, many control formulations have been applied to this problem such as neural network control (Jung, Cho and Hsia, 2007), fuzzy logic control (Zhao and Li, 2006), proportional-integral-derivative (PID) control (Nour, Ooi and Chan, 2007), sliding mode control (Demirtas, Altun and Istanbullu, 2008), H_∞ (Wu and Liu, 2007), backstepping (Ebrahim and Murphy, 2005) and model-based predictive control (Lu et al. (2007)). The related research results are widely applied in many fields, such as in military industry, space flight and robots (Gao et al. (2007)).

Model-based Predictive Control (MPC) comprises different methods such as generalized predictive control (GPC) (Clarke et al. (1987)), dynamic matrix control (DMC) (Cutler and Ramaker, 1980), predictive functional control (PFC) (Richalet et al. (1978)) among several others (Camacho and Bordons, 1999). The control law is based on the prediction, obtained by the model of the controlled process, in order to minimize the difference between the process output and the reference signal over a certain time horizon. Advantages of MPC include the possibility of handling multivariable, time-delay control problems, subject to constraints in the states and actuators. Moreover, robustness with respect to model mismatch and unmodelled dynamics can also be achieved (Maciejowski, 2002). However, there are many different formulations and many tunable parameters that need to be considered in the design of a predictive controller. Therefore, choosing the most appropriate MPC approach for a given application may not be a straightforward task. Another issue that may complicate the design of a predictive controller is the presence of multiple conflicting engineering objectives, which may not be easily translated into a single cost function.

The present paper presents a multi-objective approach for comparing and tuning some predictive control strategies employing the concepts of dominance and Pareto optimality. This approach is illustrated in a simulated case study involving the control of a single inverted pendulum coupled to a cart. Three conflicting objectives are considered, namely (1) fast response to setpoint changes in the cart position, (2) robustness with respect to model uncertainties and (3) low sensitivity to sensor noise. Two different MPC formulations are compared in terms of their Pareto boundaries for these three objectives.

The paper is organized as follows: The single inverted pendulum model is presented in Section 2. Section 3 describes the formulations of Model-based Predictive Control used in this work. Concepts related to multi-objective controller evaluation are presented in Section 4. Finally, section 5 describes the results and section 6 the conclusions.

2. SINGLE INVERTED PENDULUM

Figure 1 presents a schematic of the Single Inverted Pendulum (SIP) with two Degrees-Of-Freedom (DOF) mounted on a linear cart. The dynamic model of this system is obtained by Lagrange's method considering as the single input the cart driving force produced by the motor (F_c), and the Lagrangian coordinates (generalized coordinates) as being the cart linear position (x_c) and the pendulum angle from the upright position (α).

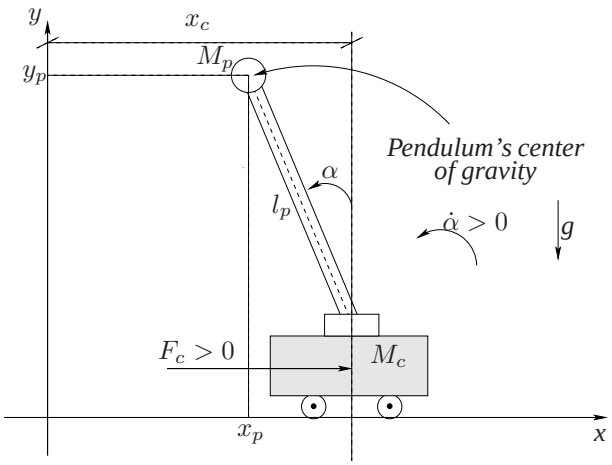

Figure 1. Description of the single inverted pendulum

This model assumes that the mass of the SIP is concentrates at its center of gravity. So, the total potential energy of the system is expressed by the following equation:

$$V_T = M_p\, g\, l_p\, cos\,(\alpha(t)) \tag{1}$$

where M_p is the pendulum mass, g is the gravity acceleration and l_p is the pendulum length from pivot to center of gravity as shown in Fig. 1.

The cart's total kinetic energy is the sum of the translational kinetic energy of the motorized cart, T_{ct}, and the rotational kinetic energy due to the cart's DC motor, T_{cr}, as expressed below:

$$\begin{aligned} T_c &= \underbrace{\frac{1}{2}\, M \left(\frac{d}{dt} x_c(t)\right)^2}_{T_{ct}} + \underbrace{\frac{1}{2} \frac{J_m\, K_g^2 \left(\frac{d}{dt} x_c(t)\right)^2}{r_{mp}^2}}_{T_{cr}} \\ &= \underbrace{\frac{1}{2} \left(M + \frac{J_m\, K_g^2}{r_{mp}^2}\right)}_{M_c} \left(\frac{d}{dt} x_c(t)\right)^2 \end{aligned} \tag{2}$$

where M is the total mass of the system, x_c is the cart linear position, J_m is the rotor moment of inertia, K_g is the planetary gearbox gear ratio and r_{mp} is the motor pinion radius.

The pendulum's total kinetic energy is the sum of the pendulum's translational kinetic energy, T_{pt}, and the pendulum's rotational kinetic energy, T_{pr}, as expressed below

$$T_p = \underbrace{\frac{1}{2}\, M_p \sqrt{\left(\frac{d}{dt}\, x_p(t)\right)^2 + \left(\frac{d}{dt}\, y_p(t)\right)^2}}_{T_{pt}} + \underbrace{\frac{1}{2}\, I_p \left(\frac{d}{dt}\, \alpha(t)\right)^2}_{T_{pr}} \tag{3}$$

where I_p is the pendulum moment of inertia with respect to the center of gravity. The linear velocity's x-coordinate and y-coordinate of the pendulum's center of gravity is determined by:

$$\begin{aligned} \frac{d}{dt}\, x_p(t) &= \left(\frac{d}{dt}\, x_c(t)\right) - l_p \cos(\alpha(t)) \left(\frac{d}{dt}\, \alpha(t)\right) \\ \frac{d}{dt}\, y_p(t) &= -l_p \sin(\alpha(t)) \left(\frac{d}{dt}\, \alpha(t)\right) \end{aligned}$$

Finally the total kinetic energy of the system is the sum of Eq. (3) and (2), which can be expressed by:

$$\begin{aligned} T_T &= \frac{1}{2}(M_c + M_p)\left(\frac{d}{dt}x_c(t)\right)^2 - M_p\, l_p \cos(\alpha(t))\left(\frac{d}{dt}\alpha(t)\right)\left(\frac{d}{dt}x_c(t)\right) + \\ &\quad \frac{1}{2}(I_p + M_p\, l_p^2)\left(\frac{d}{dt}\alpha(t)\right)^2 \end{aligned} \tag{4}$$

By definition, the two Lagrange's equations are expressed by:

$$\left(\frac{\partial}{\partial t\, \partial \frac{d}{dt}x_c(t)}(T_T - V_T)\right) - \left(\frac{\partial}{\partial x_c}(T_T - V_T)\right) = Q_{xc} \tag{5}$$

and:

$$\left(\frac{\partial}{\partial t\, \partial \frac{d}{dt}\alpha(t)}(T_T - V_T)\right) - \left(\frac{\partial}{\partial \alpha}(T_T - V_T)\right) = Q_{\alpha} \tag{6}$$

where the generalized force Q_{xc}, applied on the coordinate x_c, and the generalized force Q_α, applied on the coordinate α, can be defined as follows, neglecting the Coulomb friction applied to the linear cart and the force on the linear cart due to the pendulum's action,

$$Q_{xc}(t) = F_c(t) - B_{eq}\left(\frac{d}{dt}x_c(t)\right) \qquad \text{and} \qquad Q_\alpha(t) = -B_p\left(\frac{d}{dt}\alpha(t)\right) \tag{7}$$

where B_p and B_{eq} are the viscous damping coefficient seen by the pendulum and the motor pinion, respectively.

Finally, solving and rearranging the Lagrange's Equations (5) and (6) results in the following non-linear equations of motion of the single inverted pendulum:

$$\begin{aligned} \frac{d^2}{dt^2}x_c(t) &= \frac{-\left(I_p + M_p\, l_p^2\right)\, B_{eq}\left(\frac{d}{dt}x_c(t)\right) - \left(M_p^2\, l_p^3 + I_p\, M_p\, l_p\right)\sin(\alpha(t))\left(\frac{d}{dt}\alpha(t)\right)^2}{(M_c + M_p)\, I_p + M_c\, M_p\, l_p^2 + M_p^2\, l_p^2 \sin(\alpha(t))^2} + \\ &\quad \frac{-M_p\, l_p \cos(\alpha(t)) B_p\left(\frac{d}{dt}\alpha(t)\right) + \left(I_p + M_p\, l_p^2\right) F_c}{(M_c + M_p)\, I_p + M_c\, M_p\, l_p^2 + M_p^2\, l_p^2 \sin(\alpha(t))^2} + \\ &\quad \frac{M_p^2\, l_p^2\, g \cos(\alpha(t)) \sin(\alpha(t))}{(M_c + M_p)\, I_p + M_c\, M_p\, l_p^2 + M_p^2\, l_p^2 \sin(\alpha(t))^2} \end{aligned} \tag{8}$$

$$\begin{aligned} \frac{d^2}{dt^2}\alpha(t) &= \frac{(M_c + M_p) M_p\, g\, l_p \sin(\alpha(t)) - (M_c + M_p) B_p\left(\frac{d}{dt}\alpha(t)\right)}{(M_c + M_p)\, I_p + M_c\, M_p\, l_p^2 + M_p^2\, l_p^2 \sin(\alpha(t))^2} + \\ &\quad \frac{-M_p^2\, l_p^2 \sin(\alpha(t)) \cos(\alpha(t)) \left(\frac{d}{dt}\alpha(t)\right)^2 - M_p\, l_p \cos(\alpha(t)) B_{eq}\left(\frac{d}{dt}x_c(t)\right)}{(M_c + M_p)\, I_p + M_c\, M_p\, l_p^2 + M_p^2\, l_p^2 \sin(\alpha(t))^2} + \\ &\quad \frac{F_c\, M_p\, l_p \cos(\alpha(t))}{(M_c + M_p)\, I_p + M_c\, M_p\, l_p^2 + M_p^2\, l_p^2 \sin(\alpha(t))^2} \end{aligned} \tag{9}$$

A linearized state-space representation of Eq. (8) and (9) can be obtained by considering small departure angles, α, from the upright vertical position. For $x(t) = [\alpha\ \ x_c\ \ \dot{\alpha}\ \ \dot{x_c}]^T$ the continuous-time state-space model will be

$$\begin{cases} \dot{x}(t) &= A\, x(t) + B\, u(t) \\ y(t) &= C\, x(t) \end{cases} \tag{10}$$

where

$$A = \begin{bmatrix} 0 & 0 & 1 & 0 \\ 0 & 0 & 0 & 1 \\ 0 & \frac{g\, M_p^2\, l_p^2}{(M_c+M_p)I_p + M_c\, M_p\, l_p^2} & -\frac{B_{eq}(M_p\, l_p^2 + I_p)}{(M_c+M_p)I_p + M_c\, M_p\, l_p^2} & -\frac{M_p\, l_p\, B_p}{(M_c+M_p)I_p + M_c\, M_p\, l_p^2} \\ 0 & \frac{M_p\, g\, l_p (M_c+M_p)}{(M_c+M_p)I_p + M_c\, M_p\, l_p^2} & -\frac{M_p\, l_p\, B_{eq}}{(M_c+M_p)I_p + M_c\, M_p\, l_p^2} & -\frac{(M_c+M_p)B_p}{(M_c+M_p)I_p + M_c\, M_p\, l_p^2} \end{bmatrix}$$

$$B = \begin{bmatrix} 0 \\ 0 \\ \frac{I_p + M_p\, l_p^2}{(M_c+M_p)I_p + M_c\, M_p\, l_p^2} \\ \frac{M_p\, l_p}{(M_c+M_p)I_p + M_c\, M_p\, l_p^2} \end{bmatrix} \qquad C = \begin{bmatrix} 1 & 0 & 0 & 0 \\ 0 & 1 & 0 & 0 \end{bmatrix}$$

Finally, for $I_p = 7.88 \times 10^{-3}\, kg.m^2$, $M_c = 1.0731\, kg$, $M_p = 0.230\, kg$, $l_p = 0.3365\, m$, $B_{eq} = 5.4\, N.m.s/rad$, $B_p = 0.0024\, N.m.s/rad$ and $g = 9.81\, m/s^2$, and using a sampling time of $0.1\, s$ with a presence of a zero-order hold at the plant input, Eq. (10) can be discretized as

$$\begin{cases} x(k+1) &= A\,x(k) + B\,u(k) \\ y(k) &= C\,x(k) \end{cases} \tag{11}$$

where

$$A = \begin{bmatrix} 1 & 0.0055 & 0.059 & 0.0002 \\ 0 & 1.1277 & -0.0964 & 0.1038 \\ 0 & 0.0944 & 0.3082 & 0.0052 \\ 0 & 2.5648 & -1.6652 & 1.1194 \end{bmatrix} \quad B = \begin{bmatrix} 0.0054 \\ 0.0127 \\ 0.0909 \\ 0.2187 \end{bmatrix} \quad C = \begin{bmatrix} 1 & 0 & 0 & 0 \\ 0 & 1 & 0 & 0 \end{bmatrix}$$

3. MODEL-BASED PREDICTIVE CONTROL

The objective of the Model-based Predictive Control (MPC) is to achieve the best sequence of control actions that makes the output of the plant follow some reference signal. To do that, as shown in Figure 2, MPC employs the plant model to predict the output up to N steps ahead, where N is the prediction horizon length. Using those predictions, an optimizer computes the control sequence that minimizes a cost function and respects the constraints.

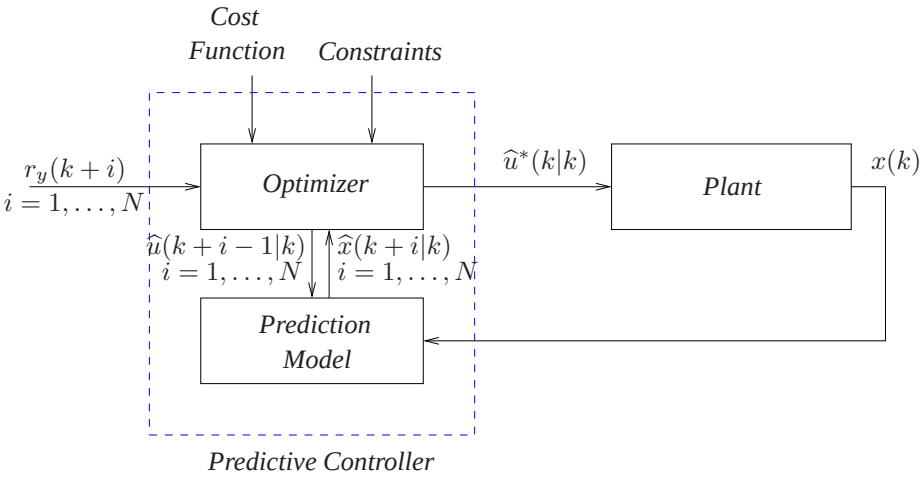

Figure 2. Discrete-time predictive controller employing state feedback

Among the several MPC formulations, this paper will be concerned with a Non-Incremental and an Incremental state-space formulation. Those techniques introduce an integrator at the plant input, in order to achieve offset-free tracking of a step reference signal (Maciejowski, 2002).

3.1 Non-incremental state-space formulation

This formulation employs the following cost function:

$$\mathcal{J} = \sum_{i=1}^{N} \left[\widehat{y}(k+i|k) - r_y(k+i)\right]^2 + \rho \sum_{i=1}^{M} \left[\Delta\widehat{u}(k+i-1|k)\right]^2 \tag{12}$$

where $\widehat{y}(k+i|k)$ is the expected output at time $k+i$ calculated on the basis of the measured state $x(k)$, M is the prediction horizon control, $\Delta\widehat{u}(k+i-1|k) = \widehat{u}(k+i-1|k) - \widehat{u}(k+i-2|k)$ is the future control increment at time $k+i-1$, $r_y(k+i)$ is the reference signal at time $k+i$ and $\rho > 0$ is a design parameter. Decreasing the value of ρ tends to increase the speed of the closed-loop response at the cost of larger control effort and greater sensitivity to measurement noise (Maciejowski, 2002).

By using the following notation:

$$Y = \begin{bmatrix} \widehat{y}(k+1|k) \\ \widehat{y}(k+2|k) \\ \vdots \\ \widehat{y}(k+N|k) \end{bmatrix} \quad R = \begin{bmatrix} r(k+1) \\ r(k+2) \\ \vdots \\ r(k+N) \end{bmatrix} \quad U = \begin{bmatrix} \widehat{u}(k|k) \\ \widehat{u}(k+1|k) \\ \vdots \\ \widehat{u}(k+M-1|k) \end{bmatrix} \quad \Delta U = \begin{bmatrix} \Delta\widehat{u}(k|k) \\ \Delta\widehat{u}(k+1|k) \\ \vdots \\ \Delta\widehat{u}(k+M-1|k) \end{bmatrix}$$

the cost function can be rewritten as

$$\mathcal{J} = (Y - R)^T (Y - R) + \rho \Delta U^T \Delta U \tag{13}$$

Considering the state-space model in Eq. (11), the relation between Y and U is of the form

$$Y = \underbrace{\begin{bmatrix} CB & 0 & 0 & \dots & 0 \\ CAB & CB & 0 & \dots & 0 \\ CA^2B & CAB & CB & \dots & 0 \\ \vdots & \vdots & \vdots & \ddots & \vdots \\ CA^{N-1}B & CA^{N-2}B & CA^{N-3}B & \dots & CB \end{bmatrix}}_{H_{N\times N}} U + \underbrace{\underbrace{\begin{bmatrix} CA \\ CA^2 \\ CA^3 \\ \vdots \\ CA^N \end{bmatrix}}_{Q_{N\times 1}} X(k)}_{F_{U_{N\times 1}}}$$

or

$$Y = H\, U + F_U \tag{14}$$

Moreover, the relation between U and ΔU can be expressed as

$$\underbrace{\begin{bmatrix} \widehat{u}(k|k) \\ \widehat{u}(k+1|k) \\ \vdots \\ \widehat{u}(k+N-1|k) \end{bmatrix}}_{U} = \underbrace{\begin{bmatrix} 1 & 0 & \cdots & 0 \\ 1 & 1 & \cdots & 0 \\ \vdots & \vdots & \ddots & \\ 1 & 1 & \cdots & 1 \end{bmatrix}}_{T_N} \underbrace{\begin{bmatrix} \Delta\widehat{u}(k|k) \\ \Delta\widehat{u}(k+1|k) \\ \vdots \\ \Delta\widehat{u}(k+N-1|k) \end{bmatrix}}_{\Delta U_{N\times 1}} + \underbrace{\begin{bmatrix} u(k-1) \\ u(k-1) \\ \vdots \\ u(k-1) \end{bmatrix}}_{1_N \cdot u(k-1)} \tag{15}$$

or

$$U = T_N\, \Delta U + 1_N\, u(k-1) \tag{16}$$

where 1_N is a column vector of N unit elements. Finally, from Eq. (14) and (16), it follows that

$$Y = \underbrace{H\, T_N}_{G_{N\times N}}\, \Delta U + \underbrace{H\, 1_N\, u(k-1) + Q\, x(k)}_{F_{N\times 1}} \tag{17}$$

or

$$Y = G\, \Delta U + F \tag{18}$$

By replacing Eq (18) in (13) the cost function can be rewritten as

$$\begin{aligned} \mathcal{J} &= \left[G\, \Delta U + F - R\right]^T \left[G\, \Delta U + F - R\right] + \rho\, \Delta U^T\, \Delta U \\ &= \Delta U^T \left[G^T\, G + \rho\, I_N\right] \Delta U + 2\, (F - R)^T\, G\, \Delta U + (F - R)^T (F - R) \end{aligned}$$

which has a minimum at

$$\Delta U^* = \left[G^T\, G + \rho\, I_N\right]^{-1}\, G^T\, (R - F) \tag{19}$$

The optimal control increment at time k is given by the first element of ΔU^*, i.e.

$$\Delta\widehat{u}^*(k|k) = K_{MPC}\, (R - F) \tag{20}$$

where

$$K_{MPC} = \underbrace{[1\ \ 0\ \ \cdots\ \ 0]}_{1\times N} \underbrace{\left[G^T\, G + \rho\, I_N\right]^{-1}\, G^T}_{N\times N}$$

Then, a discrete-time integrator is used to calculate the control to be applied to the plant:

$$\widehat{u}^*(k|k) = u(k-1) + \Delta\widehat{u}^*(k|k)$$

In usual MPC formulations, the control is kept fixed after a control horizon of M steps within the prediction horizon (Camacho and Bordons, 1999). By imposing $\Delta\widehat{u}(k+M-1|k) = 0$ for $M < i \leq N$, the last $N - M$ elements of vector

U become equal to $\widehat{u}(k+M-1|k)$. As a result, H must be replaced with matrix H_{RED}, in which the first $(M-1)$ columns are equal to the corresponding columns in H and the M^{th} column equals the sum of columns M to N of H, i.e.

$$H_{RED} = \begin{bmatrix} CB & 0 & 0 & \dots & 0 \\ CAB & CB & 0 & \dots & 0 \\ CA^2B & CAB & CB & \dots & 0 \\ \vdots & \vdots & \vdots & \ddots & \vdots \\ CA^{N-1}B & CA^{N-2}B & CA^{N-3}B & \dots & \sum_{n=M}^{N} CA^{N-M}B \end{bmatrix} \tag{21}$$

Moreover, the prediction equation (18) becomes

$$Y = G_{N\times N} \begin{bmatrix} \Delta\widehat{u}(k|k) \\ \vdots \\ \Delta\widehat{u}(k+M-1|k) \\ 0 \\ \vdots \\ 0 \end{bmatrix} + F = G_{RED} \begin{bmatrix} \Delta\widehat{u}(k|k) \\ \vdots \\ \Delta\widehat{u}(k+M-1|k) \end{bmatrix} + F$$

where G_{RED} is an $(N \times M)$ matrix corresponding to the first M columns of G. Therefore, H and G must be replaced respectively with H_{RED} and G_{RED}, in the optimal control calculations.

3.2 Incremental state-space formulation

This formulation also employs the cost function defined in Eq. (12). However, insted of using Equations (14) and (16) to obtain a prediction equation of the form (18), an incremental state-space model will be adopted. For this purpose, Eq. (11) is rewritten as

$$\begin{cases} \Delta x(k+1) &= A\,\Delta x(k) + B\,\Delta u(k) \\ \Delta y(k) &= C\,\Delta x(k) \end{cases} \tag{22}$$

where $\Delta x(k) = x(k) - x(k-1)$, $\Delta u(k) = u(k) - u(k-1)$ and $\Delta y(k) = y(k) - y(k-1)$. As shown in (Lopes, 2007), this incremental model can be used to obtain a prediction equation of the form

$$\Delta Y = H\,\Delta U + Q\,\Delta x(k) \tag{23}$$

where $\Delta Y = [\Delta\widehat{y}(k+1|k)\ \ \Delta\widehat{y}(k+2|k)\ \ \cdots\ \ \Delta\widehat{y}(k+N|k)]^T$ and H and Q matrices are those defined in the previous formulation. The relation between ΔY and Y can be expressed as

$$\underbrace{\begin{bmatrix} \widehat{y}(k+1|k) \\ \widehat{y}(k+2|k) \\ \vdots \\ \widehat{y}(k+N|k) \end{bmatrix}}_{Y} = \underbrace{\begin{bmatrix} 1 & 0 & \cdots & 0 \\ 1 & 1 & \cdots & 0 \\ \vdots & \vdots & \ddots & \\ 1 & 1 & \cdots & 1 \end{bmatrix}}_{T_N} \underbrace{\begin{bmatrix} \Delta\widehat{y}(k+1|k) \\ \Delta\widehat{y}(k+2|k) \\ \vdots \\ \Delta\widehat{y}(k+N|k) \end{bmatrix}}_{\Delta Y_{N\times 1}} + \underbrace{\begin{bmatrix} y(k) \\ y(k) \\ \vdots \\ y(k) \end{bmatrix}}_{1_N\ y(k)}$$

or

$$Y = T_N\,\Delta Y + 1_N\,y(k) \tag{24}$$

From Eq. (23) and (24),

$$Y = \underbrace{T_N\,H}_{G}\,\Delta U + \underbrace{T_N\,Q\,\Delta x(k) + 1_N \cdot y(k)}_{F}$$

i.e.,

$$Y = G\,\Delta U + F \tag{25}$$

Equation (25) is the same form of Eq. (18). Therefore, the optimal control increment can be obtained by using Eq. (20). It is worth noting that G in (25) are numerically equal to the corresponding matrices in (18). In fact, it can be shown that $T_N\,H$ (expression for G in Eq. (25)) equals $H\,T_N$ (expression for G in Eq. (18)). The only difference with respect to the previous formulation consists of the expression for the F term, which is now calculated from $\Delta x(k)$ and $y(k)$, instead of $x(k)$ and $u(k-1)$. This difference may lead to a different behaviour in the presence of sensor noise.

4. MULTI-OBJETIVE CONTROLLER EVALUATION

Most real-world problems involve multiple conflicting objectives. In such cases, improving one objective may degrade the performance in terms of one or more of the other objectives. The process of optimizing a collection of m objective functions in a simultaneous manner is called multi-objective optimization or vector optimization (Marler and Arora, 2004), which can be expressed by (Takahashi, 2007):

$$\theta^* = \arg\min_{\theta \in \mathbb{R}^n} f(\theta) \tag{26}$$

where $\theta \in \mathbb{R}^n$ is the vector of parameters that must be tuned and $f(\cdot) : \mathbb{R}^n \mapsto \mathbb{R}^m$ is a functional comprising the objectives $f_1, f_2, \ldots, f_m$.

By considering, without loss of generality, that the objective functions must be minimized, a solution $\theta^{(2)}$ is said to be dominated by $\theta^{(1)}$ if the following conditions are both satisfied:

- The solution $\theta^{(1)}$ is not worse than $\theta^{(2)}$ for all the objectives, i.e. $f_j(\theta^{(1)}) \leq f_j(\theta^{(2)})$ for all $j \in \{1, \ldots, m\}$.
- The solution $\theta^{(1)}$ is strictly better than $\theta^{(2)}$ for at least one objective, i.e. $f_j(\theta^{(1)}) < f_j(\theta^{(2)})$ for some $j \in \{1, \ldots, m\}$.

If $\theta^{(1)}$ is not dominated by any other solution $\theta \in \mathbb{R}^n$, then it is said to be non-dominated in the search space of the problem. The set of all non-dominated solutions forms the so-called Pareto-optimal boundary (or simply Pareto boundary), as illustrated in Fig. 3 for $m = 2$ objectives.

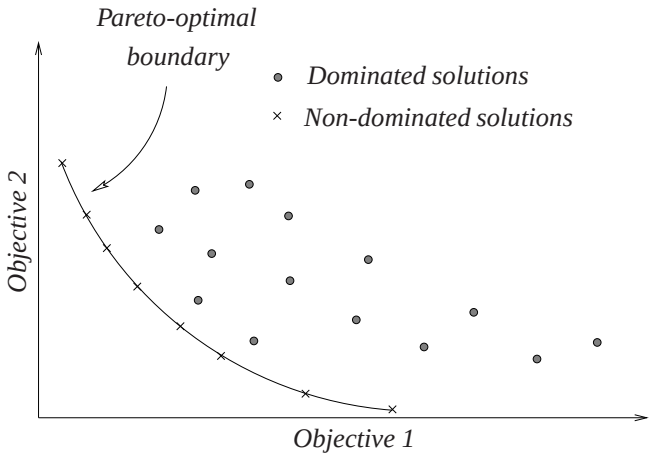

Figure 3. Pareto-optimal boundary for $m = 2$ objectives.

The solutions of the Pareto boundary are optimal in the sense that there are no better solution when all the objectives are considered simultaneously.

In this paper, $m = 3$ objectives were considered for the SIP namely: (1) fast response to setpoint changes in the cart position, (2) robustness with respect to model uncertainties and (3) low sensitivity to sensor noise. The parameter vector θ comprises the parameters N, M and ρ of the predictive controller.

The fist objective was quantified by the rise time (T_r) for a $20\,cm$ step in the set-point in the absence of measurement error and model mismatch. Moreover, T_r was determined as the time required for the plant output, y, to reach 90% of the steady-state value. The second objective, robustness with respect to model uncertainties, was quantified by the standard deviation (σ_{FAULT}) of the plant output evaluated considering a loss of 10% in the motor power. In this case, was added two quantizations that represent the tachometers actions. One of this sensor, with a step of quantization of $0.0015\,rd$, represents the tachometer of the pendulum angle. The other sensor, with a step of $2.2749 \cdot 10^{-5}\,m$, simulates the tachometer of the car position. Finally, the third objective, low sensitivity to sensor noise, was quantified by the standard deviation (σ_{NOM}) of the controlled output. It was computed by considering the angle and the position tachometers, and neglecting the model mismatch due to the loss in the motor power. For σ_{FAULT} and σ_{NOM} evaluations, the reference signal was maintained at a constant value of zero.

For each combination of N, M and ρ in the ranges $1 < M \leq N < 30$ with unit step and $0.5 < \rho < 30$ with a 0.5 step a set of non-dominated solutions was obtained for each MPC formulation using digital simulation in the *MatLab/Simulink* environment with a 4^{th} order *Runge-Kutta* solver and a fixed step size of $0.001s$. The velocities were estimated from the position readings by using second-order derivative filters with the following transfer function:

$$G(s) = \frac{62.8319^2 \cdot s}{s^2 + 2 \cdot 0.9 \cdot 62.8319 \cdot s + 62.8319^2} \tag{27}$$

5. RESULTS AND DISCUSSION

The Pareto boundaries in two-dimensional plots, obtained by the linear interpolation of the non-dominated solutions, for the two MPC formulations are presented in Figure 4. As can be seen in this figure, all of the objectives are conflicting with each other.

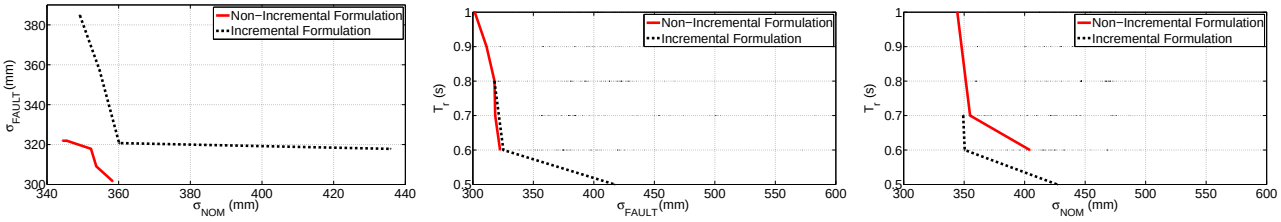

Figure 4. Two-dimensional plots for the Pareto-optimal boundaries.

Figure 5 presents the Pareto boundaries for the two MPC formulations considering the three objectives simultaneously. These boundaries were generated by cubic interpolation of the non-dominated solutions.

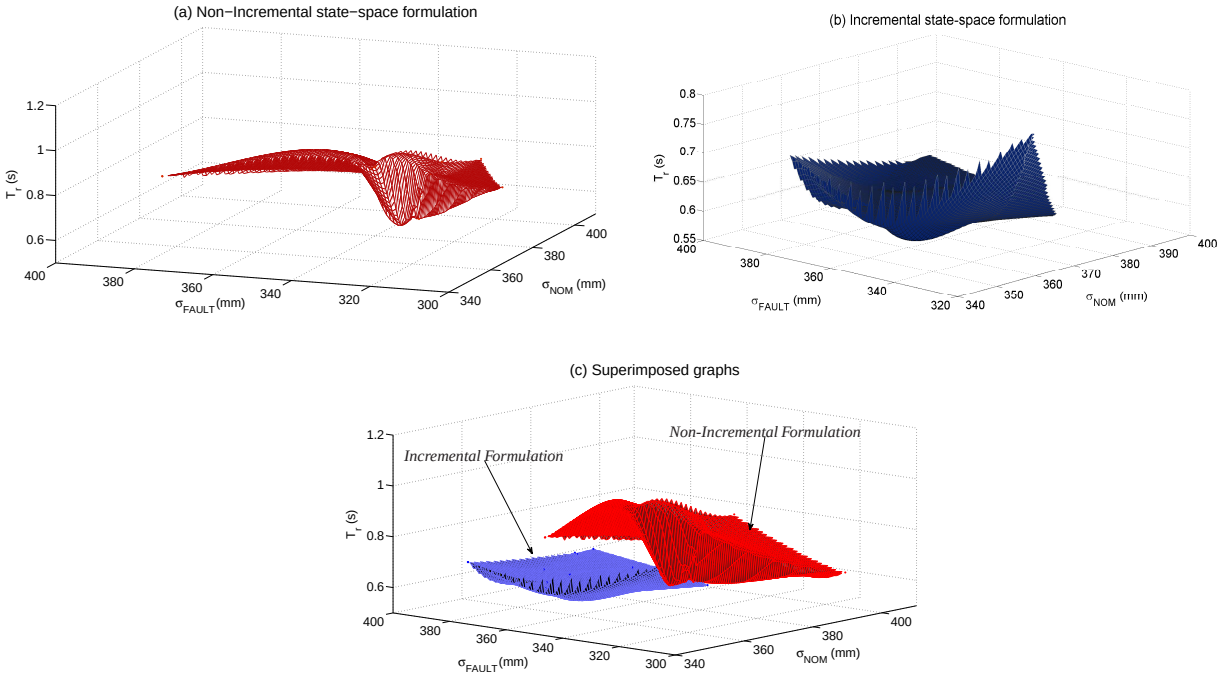

Figure 5. Pareto-optimal boundaries for Non-Incremental and Incremental state-space formulations.

A joint Pareto boundary, presented in Fig. 6, can also be generated by gathering the solutions obtained by both formulations and retaining the non-dominated ones. It is formed by merging sections of the individual boundaries shown in Figures 5a and 5b. Therefore, depending on the relative importance assigned to each objective, one MPC formulation will be more appropriate than the other.

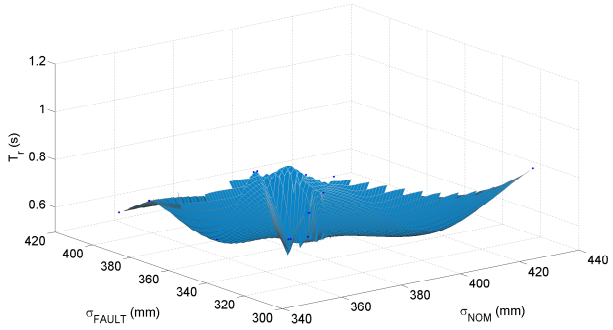

Figure 6. Joint Pareto boundary for the two MPC formulations.

Decisions concerning the choice of MPC formulations could be made by analyzing the two-dimensional plots presented in Fig 7. These plots depict projections of the joint Pareto boundary on each plane defined by a pair of objectives. The labels indicate sections corresponding to the individual Pareto boundary of each formulation.

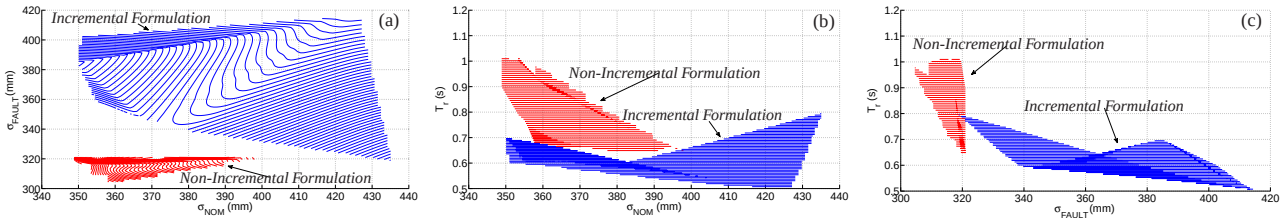

Figure 7. Projections of the joint Pareto boundary for Non-Incremental and Incremental state-space formulations.

As can be seen in Fig. 7a, the best compromise between σ_{FAULT} and σ_{NOM} is obtained by using the non-incremental state-space formulation. On the other hand, Figures 7b and 7c show that the incremental state-space formulation offers the best compromise to T_r.

An alternative visualization method consists of the use of Level Diagrams (Blasco et al., (2008)). For this purpose, each objective is normalized to the interval $[0, 1]$. The distance of the non-dominated solutions to the origin (according to a suitable norm) are then plotted against each objective and each optimization parameter. The resulting graphs, obtained by using 2-norm distances, are presented in Figure 8. Therefore, it is possible to analyse the relation between the objectives and the optimization parameters. The best compromise among the three normalized objectives can be defined as the solution closest to the origin. In this case, it is obtained by non-incremental state-space formulation with $M = 4$, $N = 7$ and $\rho = 0.5$. It is worth noting that, according to Figure 8, for $M > 11$, $1 < N < 5$ or $N > 13$, and $\rho > 2$ all the solutions are dominated.

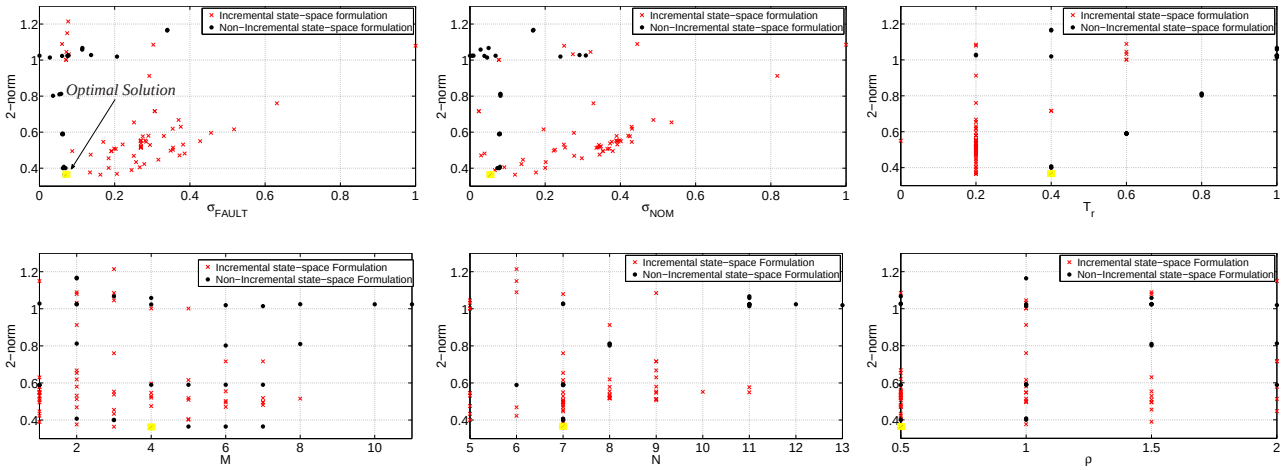

Figure 8. Level Diagrams for Incremental and Non-Incremental state-space formulations.

Other visualization strategy proposed in this work was the use of the contour plot of the spherical coordinates as shown in Fig. 9, where the color chart represents the radial distance to origin. Thus it is possible to visualize the region where is preferred the use of one formulation rather than the other one.

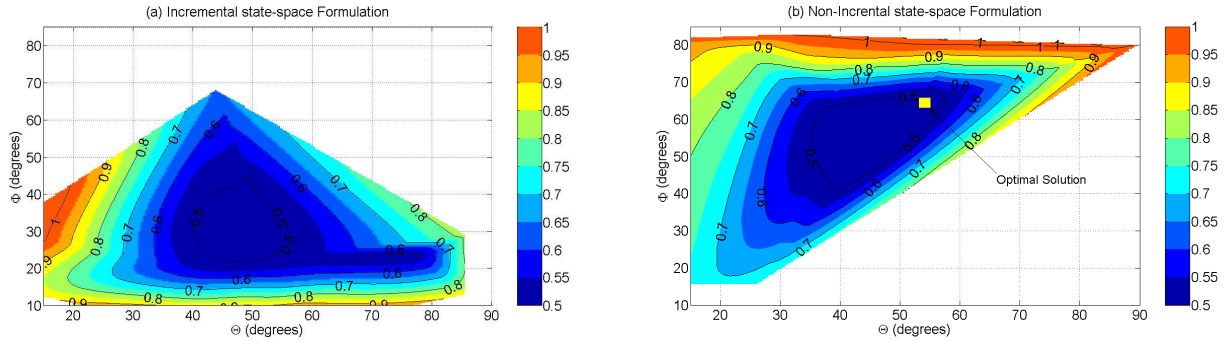

Figure 9. Contour plot of Pareto-optimal boundaries.

6. CONCLUSION

This paper presented a comparative analysis of the incremental and non-incremental state-space predictive controls formulations applied to the control of a single inverted pendulum system. By using the concept of dominated solutions

and Pareto boundaries, the comparison was carried out in terms of the performance of three conflicting objectives, namely (1) fast response to setpoint changes, (2) robustness with respect to model uncertainties and (3) low sensitivity to sensor noise, for a range of MPC tuning parameters (prediction horizon N, prediction control M and a design parameter ρ). Moreover, three methodologies for the visualization of Pareto optimal solutions were proposed to help in the decision concerning the choice of the most appropriate control formulation. The first technique is based on projections of the joint Pareto boundary on each plane defined by a pair of objectives. The second, called level diagrams, consists of representing each objective and design parameter on separate diagrams according to the distance of the non-dominated solutions to the origin. The third strategy is based on the contour plot of the Pareto boundaries represented in the spherical coordinates.

It is worth noting that when is defined the area where one formulation has a better performance than the other, using for example the projections of the joint Pareto boundary, it is possible to readjust the parameters of the controller or even switch to another control strategy in the presence of some fault in the sensors or actuators. In this paper, was analysed the performance of the system in the presence of a fault in the motor power and in the sensor.

Future works could extend this investigation by considering other control techniques (not restricted to MPC), as well as the use of different performance objectives.

7. ACKNOWLEDGMENTS

The authors acknowledge the support of FAPESP (grants 2006/58850-6 and 2007/576653), CNPq (research fellowships) and Capes/Pró-Engenharias.

8. REFERENCES

Blasco, X., Herrero, J. M., Sanchis, J., Martinez, M., 2008, “A new graphical visualization of n-dimensional Pareto front for decision-making in multiobjective optimization”. Information Sciences: an International Journal, v.178 n.20, p.3908-3924.

Camacho, E.F., Bordons, C., 1999, “Model predictive control”, Londres: Springer.

Clarke, D. W., Mohtadi, C., Tuffs, P.S., 1987, “Generalized Predictive Control”, Automatica 24, p. 137 - 169.

Cutler, C. R., Ramaker, B. L., 1980, “Dynamic Matrix Control - a computer control algorithm”, ACC, San Francisco.

Demirtas, M., Altun, Y., Istanbullu, A., 2008, “An Educational Virtual Laboratory for Sliding Mode and PID Control of Inverted Pendulum”, 11th International Conference on Optimization of Electrical and Electronic Equipment, OPTIM 2008, p. 149-156.

Ebrahim, A., Murphy, G. V., 2005, “Adaptive Backstepping Controller Design of an Inverted Pendulum”, Proceedings of the Thirty-Seventh Southeastern Symposium on System Theory, SST05, v. 37, p. 172-174.

Gao, Y., Chen, W., Lu, Z., Yu, S., 2007, “Design of Parallel Fuzzy Neural Network Controller for a Invert-Pendulum”, Second IEEE Conference on Industrial Electronics and Applications, ICIEA 2007, p. 856-861.

Jung, S., Cho, H., Hsia T. C., 2007, “Neural Network Control for Position Tracking of a Two-Axis Inverted Pendulum System: Experimental Studies”, IEEE Transactions on Neural Networks, v. 18, no. 4, p. 1042-1048.

Lopes, R. V. ,2007, “Modelagem e Controle Preditivo de um Helicóptero com três graus de liberdade.”, 136f. Dissertations(Mestrado em Sistemas e Controle)- Instituto Tecnológico de Aeronáutica, São José dos Campos.

Lu, C., Tsai, C., Tsai, M., Ling, K.V.; Yao, W., 2007, “Application of Model Predictive Control to Parallel-type Double Inverted Pendulum driven by a linear motor”, Proceedings of the 33rd Annual Conference of the IEEE Industrial Electronics Society, p. 2904-2909.

Maciejowski, J. M., 2002, “Predictive Control with Constraints”, Prentice-Hall: Harlow, England.

Marler, R.T.; Arora, J.S., 2004, “Survey of multi-objective optimization methods for engineering”, Structural and Multidisciplinary Optimization, v. 26, n. 6, p.369-395.

Nour, M. I. H., Ooi, J., Chan K. Y., 2007, “Fuzzy Logic Control vs. Conventional PID Control of an Inverted Pendulum Robot”, International Conference on Intelligent and Advanced Systems, ICIAS 2007, p. 209-214.

Richalet, J., Rault, A., Testud, J. L., Papon, J., 1978, “Model Predictive Heuristic Control: applications to industrial processes”, Automatica 14, 413 - 428.

Takahashi, R. C., 2007, “Otimização Escalar e Vetorial”, Universidade Federal de Minas Gerais, Belo Horizonte.

Wu, J., Liu, C., 2007, “Robust output-feedback control of inverted pendulum”, Second IEEE Conference on Industrial Electronics and Applications, p. 1027-1030.

Zhao, B., Li, S., 2006, “Design of a Fuzzy Logic Controller by Ant Colony Algorithm with Application to an Inverted Pendulum System”, IEEE International Conference on Systems, Man and Cybernetics, v. 5, p. 3790 - 3794.

9. Responsibility notice

The authors are the only responsible for the printed material included in this paper